J|A|C|S

JOURNAL OF THE AMERICAN CHEMICAL SOCIETY

Article

Visible-Light-Driven Rotation of Molecular Motors in a Dual-Function Metal−Organic Framework Enabled by Energy Transfer

Wojciech Danowski, Fabio Castiglioni, Andy S. Sardjan, Simon Krause, Lukas Pfeifer, Diederik Roke, Angiolina Comotti, Wesley R. Browne,* and Ben L. Feringa*

Read Online

ACCESS | Metrics & More | Article Recommendations | Supporting Information

ABSTRACT: The visible-light-driven rotation of an overcrowded alkene-based molecular motor strut in a dual-function metal−organic framework (MOF) is reported. Two types of functional linkers, a palladium−porphyrin photosensitizer and a bispyridine-derived molecular motor, were used to construct the framework capable of harvesting low-energy green light to power the rotary motion. The molecular motor was introduced in the framework using the postsynthetic solvent-assisted linker exchange (SALE) method, and the structure of the material was confirmed by powder (PXRD) and single-crystal X-ray (SC-XRD) diffraction. The large decrease in the phosphorescence lifetime and intensity of the porphyrin in the MOFs upon introduction of the molecular motor pillars confirms efficient triplet-to-triplet energy transfer between

the porphyrin linkers and the molecular motor. Near-infrared Raman spectroscopy revealed that the visible light-driven rotation of the molecular motor proceeds in the solid state at rates similar to those observed in solution.
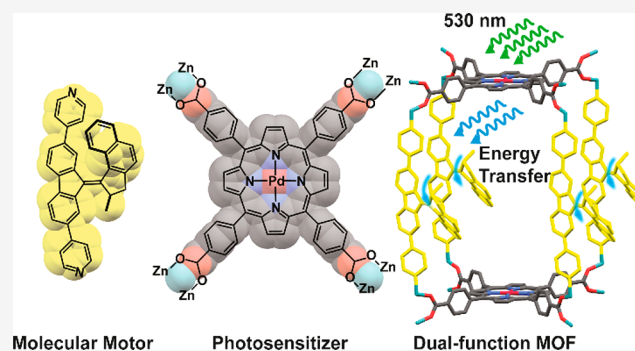
INTRODUCTION

Development of artificial molecular machines and motors allows for the design and construction of tailor-made molecular architectures capable of executing precisely controlled nano-scale structural motion.[1−8] Among these artificial systems, overcrowded alkene-based molecular motors attract considerable attention due to their chirality controlled photochemically driven repetitive unidirectional rotary motion.[9−11] Although it has been demonstrated that these molecules can perform various tasks in solution, such as control over the stereochemical outcome of catalytic reactions,[12] Brownian motion precludes the cooperative action required to achieve functions beyond molecular dimensions.[5,8,13,14] Achieving ensemble action with artificial molecular machines therefore requires that the randomizing effects of the thermal motion are eliminated by assembly on surfaces[15−17] or integration into the larger systems.[14] Incorporation and immobilization of these molecules in various supramolecular architectures, including organo-[18] and hydrogels,[19,20] polymers,[21,22] liquid crystals,[23−26] or self-assembled monolayers,[15−17] provided a way to amplify and harness their light-induced rotational motion to form responsive materials with tunable properties, including adaptive polymers,[21,22,27,28] artificial muscles,[19,20] and responsive surfaces.[29] For overcrowded alkene-based materials the use of UV light to drive the molecular motion limits such efforts due to limited penetration depth (due to the scattering) and potential damage by destructive photochemical pro-

cesses.[11,30,31] Therefore, development of reliable and practical visible-light excitation strategies that are compatible with a chosen material represents a major challenge crucial for further advancement of these dynamic systems.

The most common approaches to red shifting of the excitation wavelength of the overcrowded alkene-based molecular motors are based on HOMO−LUMO gap engineering featuring extension of the aromatic system,[32] functionalization with donor−acceptor substituents,[33,34] or formation of metal complexes.[35] Although successful, these approaches may reduce the quantum yield of photoisomerization[32] and are so far limited in the absorption shift (only to the blue part of the visible spectrum; maximum of absorption ca. 450 nm).[34] Furthermore, the resulting molecular architectures are synthetically more challenging to incorporate in a given material scaffold.[32,35,36] An alternative approach to achieve visible-light-driven rotation of these molecules is to take advantage of intra- or intermolecular sensitization through triplet energy transfer from a second chromophore.[37] This strategy not only reduces the synthetic efforts but also allows

one to tune the excitation wavelength over a broad spectral range limited only by the choice of a photosensitizer and triplet−triplet energy transfer requirements.[38] Furthermore, it has been successfully applied to operate several types of photoswitches by visible light including azobenzenes,[39,40] stilbenes,[41,42] and dithienylethenes.[43,44]

Metal−organic frameworks (MOFs) constitute a class of hybrid materials composed of inorganic nodes and organic linkers connected in a three-dimensional crystalline, highly porous network.[45−47] Due to the high inherent porosity in these structures, sufficient internal free volume is present to allow for stimuli-responsive structural transformations[48−57] or rotational[58−64] and translational[65] motion of parts of the organic linkers organized in the crystalline solid. In addition, the structural diversity and chemical tunability of these materials makes them ideal platforms to achieve spatial co-organization of functional molecules[66,67] and chromophores.[68] Recent studies on light-harvesting multicomponent MOFs revealed that facile and long-distance energy migration can be achieved between light-absorbing nodes and/or linkers in MOFs of various architectures.[69−72] Furthermore, the incorporation of photochromic dithienylethene struts in a layered porphyrin MOFs provided a method for photocontrol over energy transfer between adjacent chromophores and efficiency of singlet oxygen generation.[73,74]

Recently, we demonstrated that a molecular motor incorporated as a strut in a pillared-paddlewheel MOF is capable of performing unhindered, large-amplitude unidirectional rotary motion fueled by UV light and heat.[75] In the present study, we show that such rotary motion can be driven by visible light through linker-to-linker energy transfer. The framework was constructed from two functional linkers: a porphyrin used as both linker dictating the connectivity of the framework and light-harvesting unit and a bispyridyl-derived molecular motor serving as a pillar and able to undergo rotary motion (Figure 1). In the resulting supramolecular architecture the backbone of the framework is not only a passive "scaffolding" but also plays an active role by absorbing visible light and transferring the collected energy to the molecular motor struts, thus driving its rotary motion. This dual-function
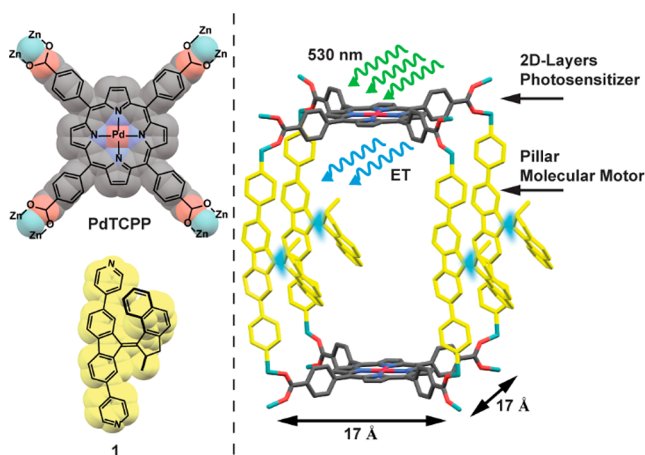

Figure 1. Structures of **PdTCPP** (left, top) and bispyridyl molecular motor **1** (left, bottom) used as linkers for construction of the MOF framework, and schematic representation of the rotation of molecular motor **1** incorporated as struts in the motorized pillared-paddlewheel **PdTCPP** MOF driven by energy transfer from a **PdTCPP** sensitizer (right). Relevant approximate dimensions of the unit cell are given.

MOF was obtained using a postsynthetic functionalization method from a parent Zn pillared-paddlewheel MOF bearing a palladium−porphyrin tetracarboxylic acid linker (**PdTCPP**) (Figure 1, top left) and bispyridyl pillars (Figure 1, bottom left). The chosen MOF scaffold provides the proximity of both linkers, allowing for efficient energy transfer between the chromophores and the large free volume that is essential for unhindered rotation of the light-driven molecular motor in the solid state (Figure 1). A key challenge, presented by this approach, is in demonstrating the functioning of the material by spectroscopic methods due to the overwhelming spectroscopic properties of the porphyrin chromophore. This unit, which is central to the visible-light-driven functionality, also precludes standard spectroscopic analysis of the motor function; however, near-infrared Raman spectroscopy (1064 nm) enables full characterization of the motor function.

■ RESULTS AND DISCUSSION

Design, Synthesis, and Characterization of a Motorized Metal−Organic Framework. For the desired MOF a zinc pillared-paddlewheel scaffold was used, related to the framework we reported recently.[75] In the chosen structure, the nodes of the framework, which is the zinc paddlewheel clusters, are connected by porphyrin tetracarboxylic acid linkers (**PdTCPP**) forming two-dimensional layers, which are pillared by the bispyridine-derived linker **1** (Figure 1). We designed the system in such a way that the size of the **PdTCPP** linker will ensure sufficient lateral separation of the pillars bearing a molecular motor function, generating free volume critical for uncompromised rotation of the molecular motor (in the designed structure, the distance between the nodes in the [100] and [010] planes is approximately 17 Å, Figure 1). Furthermore, the length of bispyridyl-derived molecular motor pillar **1** (N−N distance 15.6 Å[75]) should separate the porphyrin layers sufficiently to prevent competing interlayer porphyrin−porphyrin exciton transport. Finally, the nodes of the framework were based on closed-shell d^{10} configuration Zn^{2+} cations in order to exclude any undesired energy transfer between **PdTCPP** and nodes. Since MOFs of this topology are typically synthesized under relatively harsh conditions with the presence of strong mineral acids,[76] it was decided to prepare the final material using a postsynthetic method, i.e., solvent-assisted linker exchange (SALE) developed by Farha and Hupp.[77−81] In this process, bispyridine-derived pillars of the pillared MOFs can be exchanged for different bispyridyl linkers of similar length under neutral conditions, which prevents side reactions and decomposition of the acid-sensitive linkers.[77] Furthermore, it was demonstrated that with this method shorter pillars can also be exchanged for longer pillars, thereby making this approach suitable for fabrication of MOFs with larger unit cell parameters.[79] Initial attempts to grow the desired parent structure with N,N′-di(4-pyridyl)-1,4,5,8-naphthalenetetracarboxydiimide[75] were largely unsuccessful and gave mixtures of products consisting predominantly of interpenetrated frameworks analogous to the previously described interpenetrated porphyrinic frameworks.[82,83] To overcome this tendency of formation of the interpenetrated structure a shorter linker, meso-α,β-di(4-pyridyl) glycol (**DPG**, see Figure 2a for structure), was employed. A novel pillared-paddlewheel framework was synthesized in a solvothermal reaction between **PdTCPP**, **DPG**, $Zn(NO_3)_2 \cdot 6H_2O$, and tetrafluoroboric acid in a binary solvent mixture (DMF/EtOH) providing square-shaped crystals (Figure 2b, top). It is
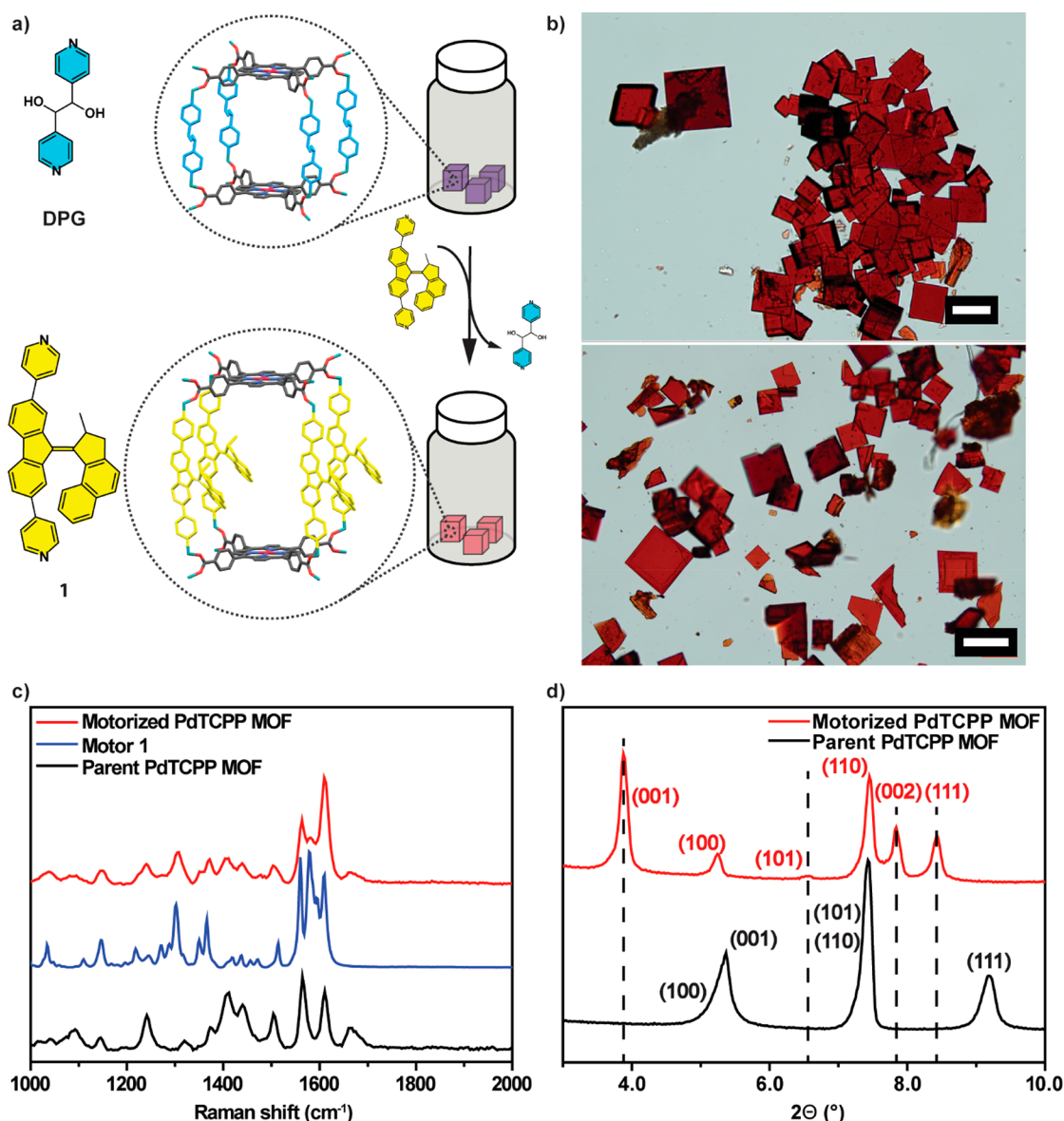
Figure 2. (a) Synthesis of the motorized pillared-paddlewheel MOF via SALE from parent MOF bearing **DPG** pillars by exchange with molecular motor **1**. (b) Optical micrograph of the parent **PdTCPP DPG**-based MOF (top) and motorized **PdTCPP 1**-based MOF (bottom) crystals obtained via linker exchange (SALE) (scale bar 100 μm). (c) Raman spectra of the parent pillared-paddlewheel MOF (black spectrum, 1064 nm, 250 mW), bispyridyl molecular motor (blue spectrum, 785 nm, 50 mW), and motorized pillared-paddlewheel MOF (red spectrum, 1064 nm, 250 mW). (d) Comparison of the experimental PXRD patterns of parent MOF (black, bottom pattern) and motorized MOF (red, top pattern). Miller indices of planes corresponding to the peaks are given in brackets. Vertical dashed lines indicate peaks in the PXRD pattern of motorized MOF, corresponding to (hkl) (where $l \neq 0$) planes.

of note that when the reaction was carried out under less acidic conditions predominantly needle-like crystals (Figure S7a) of a 3-fold interpenetrated framework with zigzag structure were obtained (Figure S7b). Characterization by ^{1}H NMR (d_6-DMSO) spectroscopy of the digested (using D_2SO_4) square-shaped crystals of the pillared-paddlewheel MOF showed the expected 1:1 ratio of **DPG** and **PdTCPP** linkers (Figures S1 and S2). The initial refinement of the single-crystal (SC) X-ray diffraction data collected from the target MOF revealed the expected layered structure composed of **PdTCPP** and **Zn** cations, while the **DPG** pillars could not be resolved, presumably due to rotational disorder (Figure S5). Nevertheless, the interlayer distance of 9.2 Å (N–N distance between pyridyl nitrogens coordinated to paddlewheel clusters) determined from the structure corresponded well

with the N–N distance (9.4 Å, see SI section 13) in the **DPG** linker, indicating that **DPG** pillars are intercalating the layers of the framework (Figure S5). The powder X-ray diffraction data (PXRD), acquired under solvent-saturated conditions, corroborated bulk crystallinity and phase purity of the sample (Figures 2d and S8). Furthermore, Pawley refinement showed negligible differences between the experimental and the simulated diffraction patterns, further indicating formation of the target pillared structure (Figures S5 and S9, Table S2). Elemental analysis corroborated the anticipated elemental composition of the parent MOF (see SI, section 2). Subsequently, the parent **DPG** pillars were exchanged for bispyridyl molecular motor **1** by means of SALE (Figure 2a), which was carried out by soaking the crystals of parent MOF in a DMF solution of bispyridyl molecular motor **1** at 80 °C for
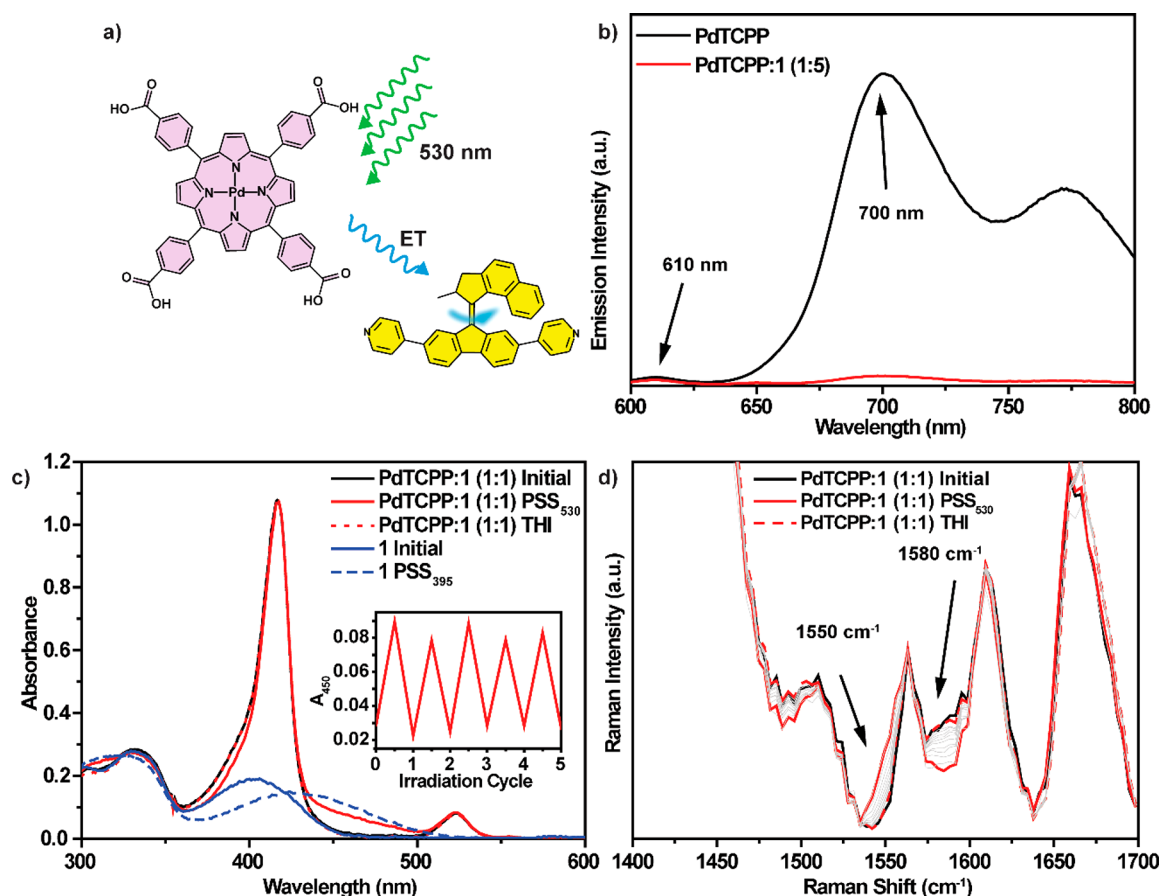
Figure 3. (a) Triplet−triplet sensitization of the light-driven rotary motion of molecular motor **1** by intermolecular energy transfer from **PdTCPP**. (b) Emission spectra (λ_{exc} = 530 nm) of **PdTCPP** (black spectrum, 44.6 μM, DMF) and a mixture of **PdTCPP** and molecular motor **1** (red spectrum, 1:5 molar ratio of **PdTCPP:1**). Emission maxima of fluorescence (610 nm) and phosphorescence (700 nm) are indicated with arrows. (c) UV−vis absorption spectra (−20 °C, 6.1 μM, DMF) of **1** (blue solid line) irradiated at 395 nm to the photostationary state (blue dashed line), a mixture of **PdTCPP** and **1** (1:1 molar ratio, black solid line), a mixture of **PdTCPP** and **1** irradiated at 530 nm to the photostationary state (red solid line), and photostationary state mixture after thermal helix inversion (red dashed line). (Inset) Changes in absorbance followed at 450 nm upon multiple irradiation and heating cycles. (d) Changes in the Raman spectrum (1064 nm, 250 mW) of a mixture of **PdTCPP** and **1** in DMF (black solid line), after irradiation at 530 nm at −20 °C to a photostationary state (red solid line), and after thermal helix inversion (red dashed line). Arrows indicate bands characteristic of the metastable isomer.

48 h (the solution of **1** was replaced with a fresh solution after 24 h) to achieve full exchange as indicated by ^{1}H NMR spectroscopy of digested crystals (Figures 2b, bottom, S1, and S3). Comparison of the Raman spectra of parent and motorized **PdTCPP** MOFs revealed the presence of additional bands characteristic of molecular motor **1** in the spectrum of motorized MOF, further supporting the successful exchange of the pillars (Figure 2c). As with the parent MOF, the SC X-ray structure of motorized MOF could only be partially resolved. From the refinement of the data the **PdTCPP** units and Zn paddlewheel clusters forming a layered structure could be confirmed, while the disorder between the layers precluded the interpretation of the electron density of the intercalating units (Figure S6). Nevertheless, the clear increase in the interlayer distance to 15.7 Å (N−N distance between pyridyl nitrogens coordinated to paddlewheel clusters) corroborated the incorporation of longer pillars, consistent with the length of the molecular motor **1** (N−N distance in DFT-optimized structure B3LYP/6-31G(d,p) 15.4 Å).[75] In addition, the expansion of the elementary unit cell in the [001] direction was confirmed by the changes observed in positions of the peaks in the PXRD diffractograms. In comparison to the PXRD of the parent MOF, significant shifts to a smaller

diffraction angle were observed for the peaks ascribed to reflections from planes perpendicular and oblique to the [001] direction, while peaks corresponding to reflections from planes parallel to the [001] direction remained unchanged (Figures 2d and S8). Furthermore, Pawley refinement showed good agreement between the dimensions of the targeted motorized **PdTCPP** MOF unit cell and the experimental PXRD pattern (Figures S8 and S9, Table S2). Finally, elemental analysis was consistent with the anticipated elemental composition of the parent MOF (see SI, section 2).

Energy Transfer, Photochemical, and Thermal Isomerization in Solution. Intermolecular energy transfer between the porphyrin (**PdTCPP**) and molecular motor **1** in solution was characterized by emission spectroscopy (Figure 3b). Deoxygenated solutions of **PdTCPP** excited at 530 nm show weak fluorescence at 610 nm and a strong emission band characteristic of phosphorescence at 700 nm (Figure 3b, black line) with a lifetime of ca. 221 μs (Figures S14−16, Table S3).[84] For mixtures of **PdTCPP** and molecular motor **1** the intensity of the phosphorescence was substantially reduced with a decrease in phosphorescence lifetime to ca. 15 μs (1:1 ratio of **PdTCPP:1**) and ca. 5 μs (1:5 ratio of **PdTCPP:1**, Figures S14−16, Table S3), in line with energy transfer

between triplet states of the porphyrin and motor **1** (Figure 3b, red line). Stern−Volmer plots (emission intensity and lifetime, Figures S14 and S16, respectively) with concentrations of **1** between 0.0 and 223.0 μM were linear, confirming dynamic quenching of the phosphorescence of **PdTCPP**, thus excluding formation of aggregates in the concentration range studied. Linear fitting of the data gave an intermolecular quenching rate constant k_q = 9.0 ± 0.3 × 10^8 M^{-1} s^{-1} approaching the Smoluchowski limit of the diffusion-limited rate constant in DMF (7.6 × 10^9 M^{-1} s^{-1} at 20 °C),[85] suggesting that the energy transfer between **PdTCPP** and **1** is likely under diffusion control (Figures S14 and S16).[86]

Intermolecular sensitization of the rotary motion of motor **1** in solution was studied with UV−vis absorption, ^{1}H NMR, and Raman spectroscopies (Figures 3c, 3d, and S4). In the UV−vis absorption spectra the region characteristic of the main absorption band of the molecular motor **1** (maximum ≈ 400 nm, Figure 3c, blue solid line) is dominated by the strong Soret band of **PdTCPP** (Figure 3c, black solid line). Nevertheless, irradiation of the argon-purged solution of **1** and **PdTCPP** (1:1 ratio of **1**:**PdTCPP**) at 530 nm (Q-band of the porphyrin) led to a bathochromic shift of the absorption in the region of the Soret band (Figure 3c, red solid line), consistent with formation of the metastable isomer of the molecular motor (Figure 3c, blue dashed lines). Subsequent warming of the sample led to the recovery of the original spectrum, consistent with the recovery of the stable isomer by thermal helix inversion (Figure 3b, red dashed line). An isosbestic point was maintained at 323 nm throughout both photochemical and thermal processes, as expected for unimolecular reactions (Figure S12). Furthermore, the irradiation/thermal isomerization cycles could be performed for at least five consecutive cycles without noticeable fatigue or degradation (Figure 3c, inset). The rate of the thermal helix inversion of bispyridyl motor **1** in the presence of **PdTCPP** in DMF was determined by following the exponential decrease of the absorbance at 440 nm over a range of temperatures (6−14 °C, Figure S13). Eyring plot analysis showed that the Gibbs free energy of activation of the thermal helix inversion of the metastable isomer of **1** in this mixture ($\Delta^{\ddagger}G$(20 °C) = 88.0 ± 0.4 kJ mol^{-1}, $t_{1/2}$ = 9.1 min, Figure S13) is essentially the same as the previously determined value in DMF[75] ($\Delta^{\ddagger}G$(20 °C) = 87.7 ± 0.6 kJ mol^{-1}, $t_{1/2}$ = 8.0 min), thereby demonstrating that bispyridyl motor **1** can operate similarly via direct excitation and triplet sensitization. In the Raman spectra of the equimolar mixture of **PdTCPP** and **1** in DMF, bands characteristic of **PdTCPP** partially overlap and obscure bands characteristic of **1** (Figure 3d, black spectrum). Nonetheless, the features consistent with sequential photochemical and thermal isomerization of **1** could be readily observed with Raman spectroscopy. Irradiation of this mixture at 530 nm at low temperature (−20 °C, sufficient to prevent thermal helix inversion over the time scale of the experiment) led to a decrease in the Raman scattering at 1580 cm^{-1} with a concomitant increase at 1550 cm^{-1}. Warming to room temperature led to gradual recovery of the initial spectrum (Figure 3d). The intermolecular energy transfer-induced photoisomerization of motor **1** was monitored with low-temperature ^{1}H NMR spectroscopy (Figure S4). After irradiation of an equimolar mixture of **1** and **PdTCPP** at 530 nm and −30 °C, a new set of upfield-shifted ^{1}H NMR resonances was observed in the aliphatic part of the spectrum, characteristic of the metastable isomer. Warming the sample

resulted in full recovery of the original spectrum and hence of the stable isomer. The photostationary state ratio of metastable and stable isomers of **1**, established upon irradiation at 530 nm, was approximately 1:1 (Figure S4), consistent with changes observed by Raman spectroscopy (Figure 3d), which showed a ∼50% decrease in the intensity of the bands characteristic of the stable isomer (1580 cm^{-1}).

Energy Transfer, Photochemical, and Thermal Isomerization in the Solid State. Since pillared Zn paddlewheel MOFs are known to lose crystallinity or undergo structural collapse upon solvent removal, all of the experiments involving **PdTCPP** MOFs were conducted in solvent (DMF)-saturated conditions.[79] The extent of the energy transfer between **1** and **PdTCPP** linkers in motorized MOF was determined with steady-state and time-resolved emission spectroscopy.

Upon excitation at 530 nm the parent **PdTCPP** MOF showed a similar emission spectrum to that of **PdTCPP** in DMF with a small hypsochromic shift of both fluorescence and phosphorescence (Figure 4a). Conversely, in the emission spectrum of the motorized **PdTCPP** MOF a strong decrease in the phosphorescence intensity was observed, consistent with the energy transfer between the linkers (Figure 4a).
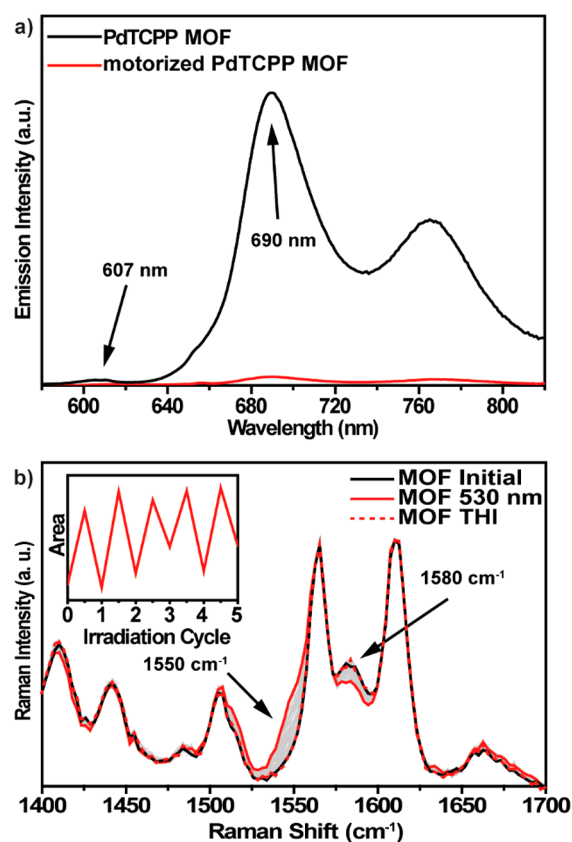
Figure 4. (a) Comparison of the emission spectra (λ_{exc} = 530 nm) of DMF suspensions of parent **PdTCPP** MOF (black line) and motorized **PdTCPP** MOF (red line). (b) Changes in the Raman spectrum (1064 nm, 250 mW, 40 s integration time) of the motorized **PdTCPP** MOF sample (black solid line) upon irradiation at 530 nm (red solid line) and subsequent thermal isomerization (red dashed line). (Inset) Changes in the area around 1550 cm^{-1} followed upon multiple photochemical/thermal isomerization cycles. Label of ordinate, "Area", refers to the integrated area between 1530 and 1551 cm^{-1}.

Furthermore, a significant drop in the porphyrin phosphorescence lifetime was observed from ca. 100 μs for the parent MOF to ca. 10 μs for the motorized MOF (Figures S17 and S18). The difference between the phosphorescence lifetimes of **PdTCPP** in solution and in the parent MOF originates from the effect of excessive scattering from the latter; nevertheless, the large decrease in emission lifetime between parent and motorized MOF clearly indicates energy transfer between **1** and **PdTCPP** linkers in MOF.

The rotary motion of motor **1** inserted in the MOF scaffold was followed with NIR−Raman spectroscopy (see SI section 12 for other spectra). Previously, we demonstrated that this technique is particularly convenient to study the photochemical and thermal isomerization of rotary molecular motors in condensed phase as it allows for unambiguous correlation of spectral data with the structural changes that these molecules exhibit in response to light and heat stimuli.[75] Upon exposure of the polycrystalline motorized **PdTCPP** MOF sample to green light (530 nm) a gradual decrease in the Raman intensity at 1580 cm^{-1} with concomitant increase in scattering intensity at 1550 cm^{-1} was observed (Figure 4b). Similar spectral features were detected upon photochemical isomerization of molecular motor **1** in solution and therefore could be ascribed to the same photochemical process. Furthermore, Raman spectroscopy showed that for thin samples the photostationary state of **1** reached via triplet sensitization in motorized **PdTCPP** MOF was similar to that in solution (Figure S22). Taking into consideration the molar absorptivity of PdTCPP at 532 nm and the concentration of molecular motor **1** in the crystal of the motorized MOF, the penetration depth for the excitation light in these crystals is likely no more than a few micrometers, and therefore, we envision the future application of these materials to be based on the surface-mounted MOFs (SURMOFs) or single-crystal devices.[87] When the irradiation was discontinued, the initial Raman spectrum was recovered gradually, indicating thermal relaxation of the metastable to stable isomer. The barrier of the thermal relaxation at room temperature was determined by monitoring the changes in the bands area characteristic of the metastable isomer (Figures S23−25 and Table S3). The Gibbs free energy of activation for this process ($\Delta^{\ddagger}G(20\ °C)$) was 88.7 ± 0.8 kJ mol^{-1} ($t_{1/2} \approx 13$ min) and corresponded well to the barrier determined in DMF solution (88.0 ± 0.4 kJ mol^{-1}, $t_{1/2} \approx 9$ min). The good agreement between the barriers in solution and the solid material shows that molecular motor **1** can perform its large amplitude rotary motion uncompromised while incorporated in **PdTCPP** MOF. Furthermore, irradiation/thermal relaxation steps could be repeated over five cycles (Figure 4b, inset) without any noticeable sign of fatigue or photodegradation, indicating high stability of the framework.

CONCLUSIONS

In conclusion, we established that the photoisomerization of the molecular motor pillars in a porphyrin Zn paddlewheel MOF can be driven with visible light by triplet sensitization. The desired motorized MOF was constructed by postsynthetic linker exchange (SALE) from the newly developed parent **PdTCPP** MOF bearing **DPG** pillars. Exchange of these pillars with the longer bispyridyl motor **1** resulted in the expected expansion of the elementary cell in the *c* direction as shown by the SC X-ray and PXRD data. Due to the spatial coarrangement of the chromophores in the motorized MOF, the energy transfer between photosensitizer (2D layers) and molecular

motor (pillars) was found to be efficient, and the photochemical isomerization of the molecular motor could be achieved with green 530 nm light. Additionally, it was shown that the rate of the thermal helix inversion step of the molecular motors incorporated in the material scaffold is essentially the same as that observed in solution, owing to the large free volume present in the framework. The demonstration of visible-light-driven rotary motion of a molecular motor in a metal−organic framework opens many perspectives for future applications, such as membranes and pumps able to accelerate flow of gases or in combination with catalytic function and miniaturized chemical reactors able to accelerate inflow of reactants and outflow of products, powered by noninvasive visible light.[88] Furthermore, we envision that this strategy may be used to expand the scope of photosensitizers and molecular motors to achieve an even further shift of the excitation wavelength toward red light.

ASSOCIATED CONTENT

Ⓢ Supporting Information

The Supporting Information is available free of charge at https://pubs.acs.org/doi/10.1021/jacs.0c03063.

Synthetic procedures and characterization, additional UV−vis and Raman spectra, Eyring plot, details on quantum yield, and lifetime determination (PDF)

X-ray crystal structure of parent **PdTCPP-DPG** MOF (CIF)

X-ray crystal structure of interpenetrated **PdTCPP-DPG** MOF (CIF)

X-ray crystal structure of motorized **PdTCPP-1** MOF (CIF)

Modeled structure of motorized **PdTCPP-1** MOF (CIF)

Modeled structure of parent **PdTCPP-DPG** MOF (CIF)

AUTHOR INFORMATION

Corresponding Authors

Wesley R. Browne − *Centre for Systems Chemistry, Stratingh Institute for Chemistry and Molecular Inorganic Chemistry Group, Stratingh Institute for Chemistry, University of Groningen, 9747 AG Groningen, The Netherlands;* ⓘ orcid.org/0000-0001-5063-6961; Email: W.R.Browne@rug.nl

Ben L. Feringa − *Centre for Systems Chemistry, Stratingh Institute for Chemistry, University of Groningen, 9747 AG Groningen, The Netherlands;* ⓘ orcid.org/0000-0003-0588-8435; Email: B.L.Feringa@rug.nl

Authors

Wojciech Danowski − *Centre for Systems Chemistry, Stratingh Institute for Chemistry, University of Groningen, 9747 AG Groningen, The Netherlands;* ⓘ orcid.org/0000-0002-8588-8912

Fabio Castiglioni − *Department of Materials Science, University of Milano Bicocca, 20125 Milan, Italy*

Andy S. Sardjan − *Molecular Inorganic Chemistry Group, Stratingh Institute for Chemistry, University of Groningen, 9747AG Groningen, The Netherlands*

Simon Krause − *Centre for Systems Chemistry, Stratingh Institute for Chemistry, University of Groningen, 9747 AG*

Groningen, The Netherlands; ● orcid.org/0000-0001-9504-8514

Lukas Pfeifer − *Centre for Systems Chemistry, Stratingh Institute for Chemistry, University of Groningen, 9747 AG Groningen, The Netherlands*

Diederik Roke − *Centre for Systems Chemistry, Stratingh Institute for Chemistry, University of Groningen, 9747 AG Groningen, The Netherlands*

Angiolina Comotti − *Department of Materials Science, University of Milano Bicocca, 20125 Milan, Italy;* ● orcid.org/0000-0002-8396-8951

Complete contact information is available at:
https://pubs.acs.org/10.1021/jacs.0c03063

■ REFERENCES

(1) Dietrich-Buchecker, C.; Jimenez-Molero, M. C.; Sartor, V.; Sauvage, J.-P. Rotaxanes and catenanes as prototypes of molecular machines and motors. *Pure Appl. Chem.* **2003**, *75*, 1383−1393.

(2) Bruns, C. J.; Stoddart, J. F. *The Nature of the Mechanical Bond: From Molecules to Machines*; Wiley: Hoboken, NJ, 2016.

(3) Balzani, V.; Venturi, M.; Credi, A. *Molecular devices and machines: a journey into the nano world*; Wiley-VCH: Weinheim, 2003.

(4) Schliwa, M. *Molecular motors*; Wiley-VCH: Weinheim, 2003.

(5) Kinbara, K.; Aida, T. Toward Intelligent Molecular Machines: Directed Motions of Biological and Artificial Molecules and Assemblies. *Chem. Rev.* **2005**, *105*, 1377−1400.

(6) Erbas-Cakmak, S.; Leigh, D. A.; McTernan, C. T.; Nussbaumer, A. L. Artificial Molecular Machines. *Chem. Rev.* **2015**, *115*, 10081−10206.

(7) García-López, V.; Liu, D.; Tour, J. M. Light-Activated Organic Molecular Motors and Their Applications. *Chem. Rev.* **2020**, *120*, 79−124.

(8) Browne, W. R.; Feringa, B. L. Making molecular machines work. *Nat. Nanotechnol.* **2006**, *1*, 25−35.

(9) Koumura, N.; Zijlstra, R. W. J.; van Delden, R. A.; Harada, N.; Feringa, B. L. Light-driven monodirectional molecular rotor. *Nature* **1999**, *401*, 152−155.

(10) Koumura, N.; Geertsema, E. M.; Meetsma, A.; Feringa, B. L. Light-driven molecular rotor: Unidirectional rotation controlled by a single stereogenic center. *J. Am. Chem. Soc.* **2000**, *122*, 12005−12006.

(11) van Leeuwen, T.; Lubbe, A. S.; Stacko, P.; Wezenberg, S. J.; Feringa, B. L. Dynamic control of function by light-driven molecular motors. *Nat. Rev. Chem.* **2017**, *1*, 96.

(12) Wang, J.; Feringa, B. L. Dynamic control of chiral space in a catalytic asymmetric reaction using a molecular motor. *Science* **2011**, *331*, 1429−1432.

(13) Astumian, R. D. Design principles for Brownian molecular machines: how to swim in molasses and walk in a hurricane. *Phys. Chem. Chem. Phys.* **2007**, *9*, 5067−5083.

(14) Coskun, A.; Banaszak, M.; Astumian, R. D.; Stoddart, J. F.; Grzybowski, B. A. Great expectations: can artificial molecular machines deliver on their promise? *Chem. Soc. Rev.* **2012**, *41*, 19−30.

(15) Carroll, G. T.; London, G.; Landaluce, T. F.; Rudolf, P.; Feringa, B. L. Adhesion of Photon-Driven Molecular Motors to Surfaces *via* 1,3-Dipolar Cycloadditions: Effect of Interfacial Interactions on Molecular Motion. *ACS Nano* **2011**, *5*, 622−630.

(16) van Delden, R. A.; ter Wiel, M. K. J.; Pollard, M. M.; Vicario, J.; Koumura, N.; Feringa, B. L. Unidirectional molecular motor on a gold surface. *Nature* **2005**, *437*, 1337−1340.

(17) Kaleta, J.; Chen, J.; Bastien, G.; Dračínský, M.; Mašát, M.; Rogers, C. T.; Feringa, B. L.; Michl, J. Surface Inclusion of Unidirectional Molecular Motors in Hexagonal Tris(o-phenylene)-cyclotriphosphazene. *J. Am. Chem. Soc.* **2017**, *139*, 10486−10498.

(18) Wezenberg, S. J.; Croisetu, C. M.; Stuart, M. C. A.; Feringa, B. L. Reversible gel−sol photoswitching with an overcrowded alkene-based bis-urea supergelator. *Chem. Sci.* **2016**, *7*, 4341−4346.

(19) Chen, J.; Leung, F. K. C.; Stuart, M. C. A.; Kajitani, T.; Fukushima, T.; van der Giessen, E.; Feringa, B. L. Artificial muscle-like function from hierarchical supramolecular assembly of photo-responsive molecular motors. *Nat. Chem.* **2018**, *10*, 132−138.

(20) Leung, F. K.-C.; van den Enk, T.; Kajitani, T.; Chen, J.; Stuart, M. C. A.; Kuipers, J.; Fukushima, T.; Feringa, B. L. Supramolecular Packing and Macroscopic Alignment Controls Actuation Speed in Macroscopic Strings of Molecular Motor Amphiphiles. *J. Am. Chem. Soc.* **2018**, *140*, 17724−17733.

(21) Li, Q.; Fuks, G.; Moulin, E.; Maaloum, M.; Rawiso, M.; Kulic, I.; Foy, J. T.; Giuseppone, N. Macroscopic contraction of a gel induced by the integrated motion of light-driven molecular motors. *Nat. Nanotechnol.* **2015**, *10*, 161−165.

(22) Foy, J. T.; Li, Q.; Goujon, A.; Colard-Itté, J. R.; Fuks, G.; Moulin, E.; Schiffmann, O.; Dattler, D.; Funeriu, D. P.; Giuseppone, N. Dual-light control of nanomachines that integrate motor and modulator subunits. *Nat. Nanotechnol.* **2017**, *12*, 540−545.

(23) Eelkema, R.; Pollard, M. M.; Vicario, J.; Katsonis, N.; Ramon, B. S.; Bastiaansen, C. W. M.; Broer, D. J.; Feringa, B. L. Nanomotor rotates microscale objects. *Nature* **2006**, *440*, 163.

(24) Pijper, D.; Jongejan, M. G. M.; Meetsma, A.; Feringa, B. L. Light-Controlled Supramolecular Helicity of a Liquid Crystalline Phase Using a Helical Polymer Functionalized with a Single Chiroptical Molecular Switch. *J. Am. Chem. Soc.* **2008**, *130*, 4541−4552.

(25) Orlova, T.; Lancia, F.; Loussert, C.; Iamsaard, S.; Katsonis, N.; Brasselet, E. Revolving supramolecular chiral structures powered by light in nanomotor-doped liquid crystals. *Nat. Nanotechnol.* **2018**, *13*, 304−308.

(26) Zou, C.; Sun, J.; Wang, M.; Wang, J.; Wu, Y.; Zhang, L.; Zhu, Z.; Xiong, G.; Jiang, L.; Ikeda, T.; Yang, H. A UV-Responsive Multifunctional Photoelectric Device Based on Discotic Columnar Nanostructures and Molecular Motors. *Adv. Mater.* **2019**, *31*, 1806016.

(27) van Leeuwen, T.; Heideman, G. H.; Zhao, D.; Wezenberg, S. J.; Feringa, B. L. In situ control of polymer helicity with a non-covalently bound photoresponsive molecular motor dopant. *Chem. Commun.* **2017**, *53*, 6393−6396.

(28) Pijper, D.; Feringa, B. L. Molecular transmission: Controlling the twist sense of a helical polymer with a single light-driven molecular motor. *Angew. Chem., Int. Ed.* **2007**, *46*, 3693−3696.

(29) Chen, K. Y.; Ivashenko, O.; Carroll, G. T.; Robertus, J.; Kistemaker, J. C. M.; London, G.; Browne, W. R.; Rudolf, P.; Feringa, B. L. Control of surface wettability using tripodal light-activated molecular motors. *J. Am. Chem. Soc.* **2014**, *136*, 3219−3224.

(30) Russew, M.-M.; Hecht, S. Photoswitches: From Molecules to Materials. *Adv. Mater.* **2010**, *22*, 3348−3360.

(31) Lubbe, A. S.; van Leeuwen, T.; Wezenberg, S. J.; Feringa, B. L. Designing dynamic functional molecular systems. *Tetrahedron* **2017**, *73*, 4837−4848.

(32) van Leeuwen, T.; Pol, J.; Roke, D.; Wezenberg, S. J.; Feringa, B. L. Visible-Light Excitation of a Molecular Motor with an Extended Aromatic Core. *Org. Lett.* **2017**, *19*, 1402−1405.

(33) van Delden, R. A.; Koumura, N.; Schoevaars, A.; Meetsma, A.; Feringa, B. L. A donor−acceptor substituted molecular motor: unidirectional rotation driven by visible light. *Org. Biomol. Chem.* **2003**, *1*, 33−35.

(34) Pfeifer, L.; Scherübl, M.; Fellert, M.; Danowski, W.; Cheng, J.; Pol, J.; Feringa, B. L. Photoefficient 2nd generation molecular motors responsive to visible light. *Chem. Sci.* **2019**, *10*, 8768−8773.

(35) Wezenberg, S. J.; Chen, K.-Y.; Feringa, B. L. Visible-Light-Driven Photoisomerization and Increased Rotation Speed of a Molecular Motor Acting as a Ligand in a Ruthenium(II) Complex. *Angew. Chem., Int. Ed.* **2015**, *54*, 11457−11461.

(36) Roke, D.; Wezenberg, S. J.; Feringa, B. L. Molecular rotary motors: Unidirectional motion around double bonds. *Proc. Natl. Acad. Sci. U. S. A.* **2018**, *115*, 9423−9431.

(37) Cnossen, A.; Hou, L.; Pollard, M. M.; Wesenhagen, P. V.; Browne, W. R.; Feringa, B. L. Driving Unidirectional Molecular Rotary Motors with Visible Light by Intra- And Intermolecular Energy Transfer from Palladium Porphyrin. *J. Am. Chem. Soc.* **2012**, *134*, 17613−17619.

(38) Perego, J.; Pedrini, J.; Bezuidenhout, C. X.; Sozzani, P. E.; Meinardi, F.; Bracco, S.; Comotti, A.; Monguzzi, A. Engineering Porous Emitting Framework Nanoparticles with Integrated Sensitizers for Low-Power Photon Upconversion by Triplet Fusion. *Adv. Mater.* **2019**, *31*, 1903309.

(39) Sakamoto, R.; Kume, S.; Sugimoto, M.; Nishihara, H. *trans - cis* Photoisomerization of Azobenzene-Conjugated Dithiolato-Bipyridine Platinum(II) Complexes: Extension of Photoresponse to Longer Wavelengths and Photocontrollable Tristability. *Chem. - Eur. J.* **2009**, *15*, 1429−1439.

(40) Venkataramani, S.; Jana, U.; Dommaschk, M.; Sonnichsen, F. D.; Tuczek, F.; Herges, R. Magnetic Bistability of Molecules in Homogeneous Solution at Room Temperature. *Science* **2011**, *331*, 445−448.

(41) Mercer-Smith, J. A.; Whitten, D. G. Photosensitization of stilbene isomerization by palladium and platinum porphyrins, an intermolecular quantum chain process. *J. Am. Chem. Soc.* **1978**, *100*, 2620−2625.

(42) Serreli, V.; Lee, C. F.; Kay, E. R.; Leigh, D. A. A molecular information ratchet. *Nature* **2007**, *445*, 523−527.

(43) Jukes, R. T. F.; Adamo, V.; Hartl, F.; Belser, P.; De Cola, L. Photochromic Dithienylethene Derivatives Containing Ru(II) or Os(II) Metal Units. Sensitized Photocyclization from a Triplet State. *Inorg. Chem.* **2004**, *43*, 2779−2792.

(44) Yam, V. W.-W.; Ko, C.-C.; Zhu, N. Photochromic and Luminescence Switching Properties of a Versatile Diarylethene-Containing 1,10-Phenanthroline Ligand and Its Rhenium(I) Complex. *J. Am. Chem. Soc.* **2004**, *126*, 12734−12735.

(45) Howarth, A. J.; Liu, Y.; Li, P.; Li, Z.; Wang, T. C.; Hupp, J. T.; Farha, O. K. Chemical, thermal and mechanical stabilities of metal-organic frameworks. *Nat. Rev. Mater.* **2016**, *1*, 1−15.

(46) Li, H.; Eddaoudi, M.; O'Keeffe, M.; Yaghi, O. M. Design and synthesis of an exceptionally stable and highly porous metal-organic framework. *Nature* **1999**, *402*, 276−279.

(47) Furukawa, H.; Cordova, K. E.; O'Keeffe, M.; Yaghi, O. M. The chemistry and applications of metal-organic frameworks. *Science* **2013**, *341*, 1230444.

(48) Jones, C. L.; Tansell, A. J.; Easun, T. L. The lighter side of MOFs: structurally photoresponsive metal−organic frameworks. *J. Mater. Chem. A* **2016**, *4*, 6714−6723.

(49) Castellanos, S.; Kapteijn, F.; Gascon, J. Photoswitchable metal organic frameworks: Turn on the lights and close the windows. *CrystEngComm* **2016**, *18*, 4006−4012.

(50) McGonigal, P. R.; Deria, P.; Hod, I.; Moghadam, P. Z.; Avestro, A.-J.; Horwitz, N. E.; Gibbs-Hall, I. C.; Blackburn, A. K.; Chen, D.; Botros, Y. Y.; Wasielewski, M. R.; Snurr, R. Q.; Hupp, J. T.; Farha, O. K.; Stoddart, J. F. Electrochemically addressable trisradical rotaxanes organized within a metal−organic framework. *Proc. Natl. Acad. Sci. U. S. A.* **2015**, *112*, 11161−11168.

(51) Chen, Q.; Sun, J.; Li, P.; Hod, I.; Moghadam, P. Z.; Kean, Z. S.; Snurr, R. Q.; Hupp, J. T.; Farha, O. K.; Stoddart, J. F. A Redox-Active Bistable Molecular Switch Mounted inside a Metal-Organic Framework. *J. Am. Chem. Soc.* **2016**, *138*, 14242−14245.

(52) Williams, D. E.; Martin, C. R.; Dolgopolova, E. A.; Swifton, A.; Godfrey, D. C.; Ejegbavwo, O. A.; Pellechia, P. J.; Smith, M. D.; Shustova, N. B. Flipping the Switch: Fast Photoisomerization in a Confined Environment. *J. Am. Chem. Soc.* **2018**, *140*, 7611−7622.

(53) Dolgopolova, E. A.; Galitskiy, V. A.; Martin, C. R.; Gregory, H. N.; Yarbrough, B. J.; Rice, A. M.; Berseneva, A. A.; Ejegbavwo, O. A.; Stephenson, K. S.; Kittikhunnatham, P.; Karakalos, S. G.; Smith, M. D.; Greytak, A. B.; Garashchuk, S.; Shustova, N. B. Connecting Wires: Photoinduced Electronic Structure Modulation in Metal-Organic Frameworks. *J. Am. Chem. Soc.* **2019**, *141*, 5350−5358.

(54) Brown, J. W.; Henderson, B. L.; Kiesz, M. D.; Whalley, A. C.; Morris, W.; Grunder, S.; Deng, H.; Furukawa, H.; Zink, J. I.; Stoddart, J. F.; Yaghi, O. M. Photophysical pore control in an azobenzene-containing metal−organic framework. *Chem. Sci.* **2013**, *4*, 2858.

(55) Furlong, B. J.; Katz, M. J. Bistable Dithienylethene-Based Metal-Organic Framework Illustrating Optically Induced Changes in Chemical Separations. *J. Am. Chem. Soc.* **2017**, *139*, 13280−13283.

(56) Zheng, Y.; Sato, H.; Wu, P.; Jeon, H. J.; Matsuda, R.; Kitagawa, S. Flexible interlocked porous frameworks allow quantitative photo-isomerization in a crystalline solid. *Nat. Commun.* **2017**, *8*, 1−6.

(57) Nikolayenko, V. I.; Herbert, S. A.; Barbour, L. J. Reversible structural switching of a metal-organic framework by photoirradiation. *Chem. Commun.* **2017**, *53*, 11142−11145.

(58) Gould, S. L.; Tranchemontagne, D.; Yaghi, O. M.; Garcia-Garibay, M. A. The Amphidynamic Character of Crystalline MOF-5: Rotational Dynamics in a Free-Volume Environment. *J. Am. Chem. Soc.* **2008**, *130*, 3246−3247.

(59) Bracco, S.; Castiglioni, F.; Comotti, A.; Galli, S.; Negroni, M.; Maspero, A.; Sozzani, P. Ultrafast Molecular Rotors and Their CO_2 Tuning in MOFs with Rod-Like Ligands. *Chem. - Eur. J.* **2017**, *23*, 11210−11215.

(60) Vogelsberg, C. S.; Uribe-Romo, F. J.; Lipton, A. S.; Yang, S.; Houk, K. N.; Brown, S.; Garcia-Garibay, M. A. Ultrafast rotation in an amphidynamic crystalline metal organic framework. *Proc. Natl. Acad. Sci. U. S. A.* **2017**, *114*, 13613−13618.

(61) Jiang, X.; Duan, H.-B.; Khan, S. I.; Garcia-Garibay, M. A. Diffusion-controlled rotation of triptycene in a metal-organic framework (MOF) sheds light on the viscosity of MOF-confined solvent. *ACS Cent. Sci.* **2016**, *2*, 608−613.

(62) Vukotic, V. N.; Harris, K. J.; Zhu, K.; Schurko, R. W.; Loeb, S. J. Metal-organic frameworks with dynamic interlocked components. *Nat. Chem.* **2012**, *4*, 456−460.

(63) Zhu, K.; Vukotic, V. N.; O'Keefe, C. A.; Schurko, R. W.; Loeb, S. J. Metal-organic frameworks with mechanically interlocked pillars: Controlling ring dynamics in the solid-state via a reversible phase change. *J. Am. Chem. Soc.* **2014**, *136*, 7403−7409.

(64) Vukotic, V. N.; O'Keefe, C. A.; Zhu, K.; Harris, K. J.; To, C.; Schurko, R. W.; Loeb, S. J. Mechanically Interlocked Linkers inside Metal - Organic Frameworks: Effect of Ring Size on Rotational Dynamics. *J. Am. Chem. Soc.* **2015**, *137*, 9643−9651.

(65) Zhu, K.; O'Keefe, C. A.; Vukotic, V. N.; Schurko, R. W.; Loeb, S. J. A molecular shuttle that operates inside a metal-organic framework. *Nat. Chem.* **2015**, *7*, 514−519.

(66) Deng, H.; Doonan, C. J.; Furukawa, H.; Ferreira, R. B.; Towne, J.; Knobler, C. B.; Wang, B.; Yaghi, O. M. Multiple Functional Groups of Varying Ratios in Metal-Organic Frameworks. *Science* **2010**, *327*, 846−850.

(67) Kong, X.; Deng, H.; Yan, F.; Kim, J.; Swisher, J. A.; Smit, B.; Yaghi, O. M.; Reimer, J. A. Mapping of Functional Groups in Metal-Organic Frameworks. *Science* **2013**, *341*, 882−885.

(68) Lee, C. Y.; Farha, O. K.; Hong, B. J.; Sarjeant, A. A.; Nguyen, S. T.; Hupp, J. T. Light-Harvesting Metal−Organic Frameworks (MOFs): Efficient Strut-to-Strut Energy Transfer in Bodipy and Porphyrin-Based MOFs. *J. Am. Chem. Soc.* **2011**, *133*, 15858−15861.

(69) Kent, C. A.; Mehl, B. P.; Ma, L.; Papanikolas, J. M.; Meyer, T. J.; Lin, W. Energy Transfer Dynamics in Metal-Organic Frameworks. *J. Am. Chem. Soc.* **2010**, *132*, 12767−12769.

(70) Zhang, X.; Ballem, M. A.; Hu, Z.-J.; Bergman, P.; Uvdal, K. Nanoscale Light-Harvesting Metal-Organic Frameworks. *Angew. Chem., Int. Ed.* **2011**, *50*, 5729−5733.

(71) Son, H.-J.; Jin, S.; Patwardhan, S.; Wezenberg, S. J.; Jeong, N. C.; So, M.; Wilmer, C. E.; Sarjeant, A. A.; Schatz, G. C.; Snurr, R. Q.; Farha, O. K.; Wiederrecht, G. P.; Hupp, J. T. Light-Harvesting and Ultrafast Energy Migration in Porphyrin-Based Metal−Organic Frameworks. *J. Am. Chem. Soc.* **2013**, *135*, 862−869.

(72) So, M. C.; Wiederrecht, G. P.; Mondloch, J. E.; Hupp, J. T.; Farha, O. K. Metal−organic framework materials for light-harvesting and energy transfer. *Chem. Commun.* **2015**, *51*, 3501−3510.

(73) Williams, D. E.; Rietman, J. A.; Maier, J. M.; Tan, R.; Greytak, A. B.; Smith, M. D.; Krause, J. A.; Shustova, N. B. Energy Transfer on Demand: Photoswitch-Directed Behavior of Metal−Porphyrin Frameworks. *J. Am. Chem. Soc.* **2014**, *136*, 11886−11889.

(74) Park, J.; Feng, D.; Yuan, S.; Zhou, H.-C. Photochromic Metal-Organic Frameworks: Reversible Control of Singlet Oxygen Generation. *Angew. Chem., Int. Ed.* **2015**, *54*, 430−435.

(75) Danowski, W.; van Leeuwen, T.; Abdolahzadeh, S.; Roke, D.; Browne, W. R.; Wezenberg, S. J.; Feringa, B. L. Unidirectional rotary motion in a metal−organic framework. *Nat. Nanotechnol.* **2019**, *14*, 488−494.

(76) Farha, O. K.; Malliakas, C. D.; Kanatzidis, M. G.; Hupp, J. T. Control over Catenation in Metal- Organic Frameworks via Rational Design of the Organic Building Block. *J. Am. Chem. Soc.* **2010**, *132*, 950−952.

(77) Madrahimov, S. T.; Atesin, T. A.; Karagiaridi, O.; Sarjeant, A. A.; Farha, O. K.; Hupp, J. T.; Nguyen, S. T. Metal-organic frameworks containing (alkynyl)gold functionalities: A comparative evaluation of solvent-assisted linker exchange, de novo synthesis, and post-synthesis modification. *Cryst. Growth Des.* **2014**, *14*, 6320−6324.

(78) Karagiaridi, O.; Bury, W.; Mondloch, J. E.; Hupp, J. T.; Farha, O. K. Solvent-assisted linker exchange: An alternative to the de novo synthesis of unattainable metal-organic frameworks. *Angew. Chem., Int. Ed.* **2014**, *53*, 4530−4540.

(79) Karagiaridi, O.; Bury, W.; Tylianakis, E.; Sarjeant, A. A.; Hupp, J. T.; Farha, O. K. Opening Metal-Organic Frameworks Vol. 2: Inserting Longer Pillars into Pillared-Paddlewheel Structures through Solvent-Assisted Linker Exchange. *Chem. Mater.* **2013**, *25*, 3499−3503.

(80) Bury, W.; Fairen-Jimenez, D.; Lalonde, M. B.; Snurr, R. Q.; Farha, O. K.; Hupp, J. T. Control over catenation in pillared paddlewheel metal-organic framework materials via solvent-assisted linker exchange. *Chem. Mater.* **2013**, *25*, 739−744.

(81) Burnett, B. J.; Barron, P. M.; Hu, C.; Choe, W. Stepwise Synthesis of Metal−Organic Frameworks: Replacement of Structural Organic Linkers. *J. Am. Chem. Soc.* **2011**, *133*, 9984−9987.

(82) Martinez-Bulit, P.; O'Keefe, C. A.; Zhu, K.; Schurko, R. W.; Loeb, S. J. Solvent and Steric Influences on Rotational Dynamics in Porphyrinic Metal-Organic Frameworks with Mechanically Interlocked Pillars. *Cryst. Growth Des.* **2019**, *19*, 5679−5685.

(83) Chung, H.; Barron, P. M.; Novotny, R. W.; Son, H. T.; Hu, C.; Choe, W. Structural variation in porphyrin pillared homologous series: Influence of distinct coordination centers for pillars on framework topology. *Cryst. Growth Des.* **2009**, *9*, 3327−3332.

(84) Vinogradov, S. A.; Wilson, D. F. Phosphorescence Lifetime Analysis with a Quadratic Programming Algorithm for Determining Quencher Distributions in Heterogeneous Systems. *Biophys. J.* **1994**, *67*, 2048−2059.

(85) Montalti, M.; Credi, A.; Prodi, L. P.; Gandolfi, M. T. *Handbook of photochemistry*, 3rd ed.; CRC/Taylor & Francis: Boca Raton, 2006.

(86) Lakowicz, J. R. *Principles of fluorescence spectroscopy*; Lakowicz, J. R., Ed., Springer: Boston, MA, 2006.

(87) Heinke, L.; Wöll, C. Surface-Mounted Metal-Organic Frameworks: Crystalline and Porous Molecular Assemblies for Fundamental Insights and Advanced Applications. *Adv. Mater.* **2019**, *31*, 1806324.

(88) Evans, J. D.; Krause, S.; Feringa, B. L. Cooperative and synchronized rotation in motorized porous frameworks: Impact on local and global transport properties of confined fluids. *Faraday Discuss.* **2020**. DOI: 10.1039/D0FD00016G